J. Plasma Physics (2002), *vol.* 67, *parts* 2&3, *pp.* 149–161.
DOI: 10.1017/S0022377801001301 Printed in the United Kingdom

Modified electron whistler dispersion law

B. V. LUNDIN[1] and C. KRAFFT[2]

[1]Institute of Terrestrial Magnetism, Ionosphere and Radiowave Propagation, Russian Academy of Sciences, Troitsk, Moscow Region, 142190, Russia

[2]Laboratoire de Physique des Gaz et des Plasmas, Université Paris-Sud, 91405 Orsay Cedex, France

(Received 21 February 2001)

Abstract. A modified electron whistler dispersion law is derived in the cold-plasma approximation for analytical treatment and simplified numerical calculations of wave propagation in a wide range of ratios ω_c/ω_p of electron gyro- to plasma frequencies if the wave frequency is much less than ω_p. The net contribution of ions to the wave dispersion law is expressed through the value of the lower-hybrid resonance frequency ω_{lhr} only. This approximate dispersion law is valid in a wide frequency domain, that is, from the range of ω_{lhr} until the domain where the contribution of ions can be neglected. A comparison of geometrical-optics ray trajectories calculated by the use of modified and total cold-plasma electron whistler dispersion laws is presented for the case of the Earth's plasma environment. Computer simulations of dynamical spectra of whistler waves excited by lightning discharges and registered in remote regions of the Earth's plasmasphere reveal good numerical stability of the developed ray-tracing code.

1. Introduction

The use of geometrical optics (GO) (Felsen and Marcuvits 1973; Kravtsov and Orlov 1980) is in many cases an effective approach to obtaining approximate relevant solutions of Maxwell's equations in space plasma conditions (see e.g. Kimura 1985); moreover, it can be applied fruitfully to the analysis of wave-plasma interaction in laboratory devices (Petrov et al. 2000).

In the near-Earth plasma environment, the typical applications related to passive or active low-frequency electromagnetic sounding are connected with electron whistler mode waves (Helliwell 1993). Such waves are registered hourly on the Earth's surface as well as on board satellites or space vehicles moving in the vicinity of planets; they can propagate over distant regions of planetary magnetospheres, being well guided by geomagnetic field lines (Helliwell 1965, 1993). In particular, they play an important role in establishing the equilibrium state of radiation belts (Kennel and Petschek 1966). Even if the typical source of whistlers is lightning discharges, several types of plasma instabilities can also give rise to whistler mode emissions. Moreover, recent developments in helicon discharge physics are also connected with the interaction of non-plane waves of the electron whistler mode with a bounded plasma in finite-size laboratory devices (Boswell and Chen 1997; Chen and Boswell 1997).

GO equations have been fruitfully used for interpreting electron whistler spectrograms (i.e. dynamical frequency–time spectra) registered in overdense plasmaspheric plasmas extending typically out to a few Earth radii. In this way, the propagation of quasi monochromatic wave packets between emitters and remote receivers through an intermediate background plasma with large-scale inhomogeneities was investigated. Another natural application is connected with the study of the modification of wide electromagnetic spectra emitted by natural impulsive and extended sources such as lightning discharges due to the essential scattering of ray trajectories on their path to the remote receiver, so that some wavepackets are unable to reach the receiver.

One of the typical difficulties arising when solving GO equations is the so-called 'aiming problem', i.e. the necessity to select starting conditions for rays such that they are able to reach a given target or illuminate a remote receiver, for example. There is no rapid general way to achieve this aim, especially when considering space plasmas with curvilinear magnetic field lines and very wide ranges of variation of characteristic parameters. Even though the power of modern personal computers allows one, in some limited cases, to partly solve such problems in a reasonably short computing time by direct enumeration of all possible meaningful ray starting conditions, to reach this goal necessitates simplification of the dispersion equation for waves of the considered plasma mode. The direct use of the general total cold-plasma dispersion law requires more computer resources, and also often encounters the problem of numerical instability, which is connected with very large variations of background plasma parameters along ray trajectories, In fact, we have found that a numerical code of the same structure based on a simplified dispersion law is more stable.

To derive a relevant simplified dispersion law for electron whistlers propagating in very wide relative frequency domains (with respect to background plasma characteristic frequencies) is a rather complex problem, even when considering the limiting case of the cold-plasma approximation. Indeed, for the typical Earth plasma environment and a fixed frequency, one should take into account the contribution to the dielectric permittivity tensor of several plasma components with very different altitude scales in their space distributions, the steep variation of the dipole-like magnetic field with radius, and, as a result, the very wide range of ratios of wave frequency to the characteristic frequencies of the background plasma crossed by the rays. The inherent accompanying problem consists in choosing an adequate model of particle density distributions with altitude. Nevertheless, for wave frequencies much less than the plasma frequency, we have found a relevant approximate dispersion law that retains the features of the total cold-plasma whistler dispersion equation in very wide frequency domains, that is, from the range of the so-called lower-hybrid resonance (LHR) frequency ω_{lhr} until the domain where the contribution of ion motion can be neglected. In this limit, the net combined contribution of all ions is expressed through the LHR frequency only; this reduces the amount of background plasma parameters needed for the calculations, and enables one, in principle, to use the spectrogram records of intense LHR frequency emissions by satellites for adequate fitting of the model in use.

This paper is organized as follows. In the next section, we derive the modified whistler dispersion law valid in a wide frequency domain, which can be 'naturally' reduced to the conventional one (see (20), and Shafranov 1967) corresponding to high-frequency whistler waves of high refractive index in an overdense plasma when

the plasma frequency ω_p is much larger than the electron gyrofrequency ω_c. Expressions for group velocity and frequency gradient are presented in the Appendix, where the 'infinity problem' for radiation energy loss of Cherenkov electrons inherent to the conventional dispersion law is also discussed. In order to demonstrate the relevance of our approximation, a comparison between ray trajectories calculated by the simplified and the total dispersion laws is presented in Section 3. Finally, simulations of the so-called magnetospherically reflected whistler spectrograms are presented in order to illustrate one possible example of application.

2. Modified whistler dispersion law

The dispersion equation for waves propagating in a cold plasma can be written without any approximation as follows:

$$\cos^2\theta\left(1-\frac{\chi}{N^2}\right)=\left(1-\frac{\eta}{N^2}\right)\left[\cos^2\theta_R\left(1-\frac{\eta}{N^2}\right)-\frac{\chi}{N^2}\right], \tag{1}$$

where $N = ck/\omega$ is the refractive index, c the speed of light, k the wavenumber modulus, ω the frequency, and θ the angle between the wave vector $\mathbf{k}$ and the background magnetic field $\mathbf{B}_0$ ($\cos\theta \equiv \mathbf{k}\cdot\mathbf{B}_0/kB_0$). Expressions for χ and $\cos^2\theta_R$, actually corresponding to formal definition of the resonance angle θ_R, i.e. $\varepsilon\sin^2\theta_R + \eta\cos^2\theta_R = 0$, can be written as (for $\cos^2\theta_R < 0$, the resonance cone does not exist for plane waves)

$$\chi \equiv \varepsilon - \frac{g^2}{\varepsilon-\eta}, \qquad \cos^2\theta_R \equiv \frac{\varepsilon}{\varepsilon-\eta}. \tag{2}$$

The components ε, g and η of the dielectric permittivity tensor in a cold plasma (Shafranov 1967) are defined by

$$\varepsilon = 1-\sum_\alpha \frac{\omega_{p\alpha}^2}{\omega^2-\omega_{c\alpha}^2}, \qquad g = -\sum_\alpha \frac{\omega_{p\alpha}^2\omega_{c\alpha}}{\omega(\omega^2-\omega_{c\alpha}^2)}, \qquad \eta = 1-\sum_\alpha \frac{\omega_{p\alpha}^2}{\omega^2}, \tag{3}$$

where $\omega_{p\alpha}$ and $\omega_{c\alpha}$ are the plasma frequency and gyrofrequency of species α, respectively; for electrons, one uses the notation $\omega_p \equiv \omega_{pe}$ and $\omega_c \equiv -\omega_{ce} > 0$.

The presentation of the dispersion law in the form (1) is rather natural for waves of high refractive index; at the same time, the coefficients χ, η and $\cos^2\theta_R$ depend on the frequency only (and not on θ). An additional simplification can be achieved in the high-frequency limit, when ion motion can be neglected; in this case, one has

$$\chi = 1, \qquad \cos^2\theta_R = \frac{\omega^2}{\Omega_c^2}\left(1-\frac{\omega^2}{\omega_p^2+\omega_c^2}\right) \tag{4}$$

with

$$\Omega_c^2 = \frac{\omega_c^2}{1+\mu}, \qquad \mu = \frac{\omega_c^2}{\omega_p^2}, \tag{5}$$

(see also Stix 1992). In the low-frequency limit $\omega \ll \omega_c$ and for frequencies greater than the maximum ion gyrofrequency i.e. $\omega \gg \omega_H$ (where ω_H is the hydrogen-ion gyrofrequency), keeping the main terms in (3) leads to

$$\chi \simeq \tilde{\chi} = 1-\frac{1+\mu}{\mu}\frac{\omega_{lhr}^2}{\omega^2}, \qquad \cos^2\theta_R \simeq \cos^2\tilde{\theta}_R = \frac{\omega^2}{\Omega_c^2}\left(1-\frac{\omega_{lhr}^2}{\omega^2}\right), \tag{6}$$

where the small terms $\omega_H/\omega_c \ll 1$ have been omitted; the approximation $\eta \simeq$

https://doi.org/10.1017/S0022377801001301 Published online by Cambridge University Press

$-\omega_p^2/\omega^2$ was used when ω_p is not very small compared with ω_c, so that the relation $\omega^2 \ll \omega_p^2$ results from $\omega^2 \ll \omega_c^2$. Finally, a simplified dispersion equation can be obtained as

$$\cos^2\theta\left(1-\frac{\tilde{\chi}}{N^2}\right)=(1+\kappa)\frac{\omega^2}{\Omega_c^2}\left(1-\frac{\omega_{lhr}^2}{\omega^2}+\tilde{\kappa}\right), \tag{7}$$

with

$$\Omega_p^2=\frac{\omega_p^2}{1+\mu}, \qquad \kappa=\frac{\omega_p^2}{k^2c^2}, \qquad \tilde{\kappa}=\frac{\Omega_p^2}{k^2c^2}. \tag{8}$$

This dispersion law follows from (1) in the frequency domain $\omega_H \ll \omega \ll \{\omega_c, \omega_p\}$, where the ratio ω_c^2/ω_p^2 is not limited to small values; the lower-hybrid resonance frequency $\omega_H \ll \omega_{lhr} \ll \omega_c$ satisfies the condition $\varepsilon = 0$, and can be found from the usual expression

$$\omega_{lhr}^2 \equiv \frac{\mu}{1+\mu}\sum_\alpha \omega_{p\alpha}^2 = \frac{\omega_H\omega_c}{1+\mu}M_{\text{eff}}^{-1}, \tag{9}$$

$$M_{\text{eff}}^{-1} \equiv \sum_\alpha \frac{n_\alpha}{n_e}\frac{M_H}{M_\alpha}, \qquad \omega_p^2 \equiv \frac{4\pi n_e e^2}{m_e}, \qquad \omega_{p\alpha}^2 \equiv \frac{4\pi n_\alpha e_\alpha^2}{M_\alpha}, \qquad \omega_{pi}^2=\sum_\alpha \omega_{p\alpha}^2, \tag{10}$$

where α labels the different ions; n_α, e_α and M_α are the density, charge and atomic mass of species α ($M_H = 1$); subscript e (respectively H) corresponds to electrons (respectively the hydrogen ion); M_{eff} is an effective ion mass expressed in atomic mass units; ω_{pi} is the ion plasma frequency.

In the high-frequency limit, which is realized for frequencies much greater than the ion plasma frequency $\omega \gg \omega_{pi}$, (4), the dispersion equation can be obtained from (7) by omitting terms containing ω_{lhr} and putting $\tilde{\chi} = 1$, that is

$$\cos^2\theta\left(1-\frac{\omega^2}{k^2c^2}\right)=(1+\kappa)(1+\tilde{\kappa})\frac{\omega^2}{\Omega_c^2}. \tag{11}$$

Using (7) (or (11)), one can find the frequency as a function of the wave vector; then one obtains from (7) that

$$\omega^2[(1+\kappa)(1+\tilde{\kappa})+\mu\tilde{\kappa}\cos^2\theta]=\Omega_c^2\cos^2\theta+\omega_{lhr}^2(1+\kappa+\kappa\cos^2\theta). \tag{12}$$

Let us mention that a very similar dispersion law for the low-frequency domain $\omega_H \ll \omega \ll \omega_c$ has been presented before by Bud'ko (1985); however, the expression of Bud'ko keeps the superfluous small terms $\omega_{pi}^2/\omega_p^2 \ll 1$, which should be omitted together with $\omega_{lhr}^2/\omega_c^2 \ll 1$; then its corrected form coincides with (12). One should note that the upper part of the frequency range $\omega_H \ll \omega \ll \{\omega_c, \omega_p\}$ for validity of (7), namely $\omega_{lhr} < \omega_{pi} \ll \omega \ll \{\omega_c, \omega_p\}$, overlaps with the validity range of (11), namely $\omega_{pi} \ll \omega \ll \omega_p$. In the upper part of these frequency ranges, the approximate expressions for the coefficients χ and $\cos^2\theta_R$ of both equations differ from each other by negligibly small terms of the order of $(\omega_{pi}/\omega)^2$. Then it is rather natural to accept (7) (or (12)) as an appropriate approximation for the electron whistler dispersion law valid in the total frequency domain $\omega_H \ll \omega \ll \omega_p$. The possibility of a smooth transition from the coefficients (6) to the expressions (4) is based on the existence of a large domain $\omega_{pi} \ll \omega \ll \omega_c$ of common applicability if ω_{pi}^2/ω_c^2 is small enough that

$$\frac{m_e}{M_H}\frac{\omega_p^2}{\omega_c^2}M_{\text{eff}}^{-1} \ll 1. \tag{13}$$

https://doi.org/10.1017/S0022377801001301 Published online by Cambridge University Press

The other condition for appropriate plasma parameters can be found from the relation $\omega_H \ll \omega_{lhr}$; actually it is easy to satisfy

$$\left(1 + \frac{\omega_c^2}{\omega_p^2}\right) \frac{m_e}{M_H} M_{\text{eff}} \ll 1, \tag{14}$$

except for the case of a very rarefied plasma, when

$$\frac{\omega_p^2}{\omega_c^2} \lesssim \frac{m_e}{M_H} M_{\text{eff}}. \tag{15}$$

An additional simplification of (7) can be useful for the analytical treatment of dispersive properties of electron whistler waves. This can be achieved for high values of the refractive index, $\chi N^{-2} \ll 1$, so that the simplified dispersion law takes the following form (here one should omit in (12) terms containing $\kappa \cos^2\theta$ and $\tilde{\kappa} \cos^2\theta$):

$$\omega^2 = \frac{\omega_{lhr}^2}{1 + \tilde{\kappa}} + \frac{\Omega_c^2 \cos^2\theta}{(1 + \kappa)(1 + \tilde{\kappa})}. \tag{16}$$

For small values of κ and $\tilde{\kappa}$, the quasiresonant regime of propagation can be realized for angles θ close to the resonant cone angle θ_R:

$$\cos^2\theta_R = \frac{\omega^2}{\omega_c^2}\left(1 + \frac{\omega_c^2}{\omega_p^2}\right) - \frac{m_e}{M_H} M_{\text{eff}}^{-1}. \tag{17}$$

In the high-frequency limit $\omega^2 \gg \omega_{lhr}^2$, the expression (16) differs negligibly from that obtained directly from (1), when ion motion is neglected ($\chi = 1$, $N^{-2} \ll 1$ and $\omega \ll \omega_p$ so that (4) reduces to $\cos^2\theta_R = \omega^2/\Omega_c^2$).

Actually, the condition $N^{-2} \ll 1$ can be written by use of (16) as

$$\frac{1}{N^2} = \mu \frac{\tilde{\kappa}}{1 + \tilde{\kappa}} \left(\frac{\cos^2\theta}{1 + \kappa} + \frac{m_e}{M_H} M_{\text{eff}}^{-1}\right) \ll 1, \tag{18}$$

and is naturally satisfied under overdense plasma conditions, when $\mu \ll 1$; however, for $\mu \simeq 1$, the dispersion law (16) is valid for $\tilde{\kappa} \cos^2\theta \ll 1$.

The high-frequency modified dispersion law for electron whistlers can be found from (12) by omitting terms containing ω_{lhr}:

$$\omega^2 = \frac{\Omega_c^2 \cos^2\theta}{(1 + \kappa)(1 + \tilde{\kappa}) + \mu\tilde{\kappa} \cos^2\theta}. \tag{19}$$

We remind the reader that the term in (19) containing $\mu\tilde{\kappa}$ is a direct consequence of the term ω^2/k^2c^2 on the left-hand side of (11), which is not considered here as small in comparison with unity. Under overdense plasma conditions ($\mu \ll 1$), one recovers the conventional whistler dispersion law ($\tilde{\kappa} \simeq \kappa$, $\Omega_c^2 \simeq \omega_c^2$):

$$\omega^2 = \frac{\omega_c^2 \cos^2\theta}{(1 + \kappa)^2}. \tag{20}$$

Thus, we have demonstrated that, for electron whistler waves with frequencies $\omega_H \ll \omega \ll \omega_p$, the simplified dispersion law presented in (7) and solved in the form (12) is a relevant approximation of the total cold-plasma dispersion law in a wide frequency domain including the LHR frequency range in its lower part as well as the high-frequency domain where ion motion can be neglected. The possible plasma density should satisfy the conditions (13) and (14); both are easy to fulfil because of the smallness of the parameter $m_e/M_H \simeq 5 \times 10^{-4}$.

https://doi.org/10.1017/S0022377801001301 Published online by Cambridge University Press

Let us briefly discuss some additional questions that can arise when applying (19) to quasiresonant whistler waves of the highest possible frequencies. It is known from cold-plasma theory that the resonant ($\kappa \simeq 0$) frequency corresponding to $\cos^2\theta_R = 1$ should be equal to the minimum value of $\{\omega_c, \omega_p\}$. However, according to (19), the resonance should occur at a frequency $\mathbf{\Omega}_c = \omega_c/\sqrt{(1+\omega_c^2/\omega_p^2)}$; then to satisfy at $\omega \simeq \mathbf{\Omega}_c$ the validity condition (19), i.e. $\omega \ll \omega_p$, one needs overdense plasma conditions $\omega_c^2/\omega_p^2 \ll 1$. Thus, the vicinities of resonant points $\cos^2\theta \simeq \cos^2\theta_R \simeq 1$ at the highest frequencies in space regions where $\omega_c \gtrsim \omega_p$ are not described by the approximation (19). This means that when applying (12) to GO equations in space plasmas (as will be done below), one should discard those solutions corresponding to rays that reach the regions where the local condition $\omega \ll \omega_p$ is not fulfilled. The origin of this problem lies in the fact that the component of the displacement current parallel to $\mathbf{B}_0$ for low-frequency waves is neglected throughout the paper, so that $\eta = -\omega_p^2/\omega^2$.

In the next section, we actually compare numerically ray trajectories satisfying the conditions $10\omega_H^2 \leqslant \omega^2 \leqslant \frac{1}{10}\omega_p^2$ and calculated using either the full cold-plasma dispersion law or the simplified one (12), under typical conditions corresponding to the so-called diffusive equilibrium density distributions in the near-Earth plasma environment. Spatial distortions between ray trajectories calculated by both dispersion laws are shown to be not significant for any kind of trajectories. However, the corresponding relative difference in arrival time for almost-coinciding trajectories can reach 10–20%; this is not surprising, especially for the case of quasiresonant ray trajectories with high refractive index, when the group velocity tends to zero, with an almost-fixed direction of propagation close to the resonance cone. Moreover, the numerical stability of solutions (e.g. the accuracy of frequency conservation along the ray) of GO equations is typically better when using the approximate dispersion law (12) than the full cold-plasma dispersion law.

3. Application to wave propagation in space plasmas

3.1. Numerical analysis of ray trajectories

Let us compare with each other several ray trajectories of qualitatively different kinds calculated in inhomogeneous plasmas with very large scattering of characteristic parameters inherent to the wide space regions where rays propagate. An appropriate sample is the near-Earth plasma, where $\omega_c \simeq \omega_p \simeq 1\,\mathrm{MHz}$ and $\omega_{lhr} \simeq 10\,\mathrm{kHz}$ at altitudes $h \simeq 1000\,\mathrm{km}$; however, at radial distances of around $4R_E$ (where R_E is the Earth's radius), the electron gyrofrequency at the equator is around $\omega_{ceq} \simeq 13.5\,\mathrm{kHz}$, whereas $\omega_p > 20\omega_c$, and $\omega_{lhr} \simeq 0.3\,\mathrm{kHz}$, depending on features of altitude density distributions. Thus, a ray with frequency $\omega \simeq 13.8\,\mathrm{kHz}$ belongs to the near-LHR frequency range at $h \simeq 1000\,\mathrm{km}$, but it has a relatively high frequency near ω_c at $h \simeq 20\,000\,\mathrm{km}$.

In order to demonstrate quantitatively the relevance of the dispersion-law approximation, let us first present different kinds of whistler ray trajectories calculated using either the total cold-plasma whistler dispersion law or the simplified one (12), in the Earth's plasmasphere as well as outside it. The plasmasphere is the dense plasma surrounding the Earth, which rotates together with it; its outer boundary (called the plasmapause) corresponds to a steep drop-off of the plasma density almost across the geomagnetic field lines, forming a gradient-type waveguide along the magnetic shell at an equatorial radial distance of around $4R_E$,

https://doi.org/10.1017/S0022377801001301 Published online by Cambridge University Press

that is at $L \simeq 4$, where L is the so-called McIllwain or L-shell parameter. Taking into account the large steep increase of conductivity at the lower boundary of the ionosphere, it is commonly accepted that the wave vector of starting whistler wave packets excited by lightning discharges is oriented almost vertically (Edgar 1976). A dipole-like magnetic field structure was used and the altitude distributions of particle densities were chosen in accordance with the so-called diffusive equilibrium model where the charged particles (electrons and two main ions: hydrogen and oxygen) are distributed in the Earth's gravitational field according to a Boltzmann law, essentially modified by the particles' mutual Coulomb interaction providing the net quasineutrality of the plasma (Angerami and Thomas 1964).

Figure 1 shows typical doubled rays – that is, the two ray trajectories calculated with the use of total and simplified dispersion laws – influenced by large-scale inhomogeneities of the magnetic field and the plasma environment, as well as by the drop-off of the plasma density at the plasmapause near $L \simeq 4$ (see also Inan and Bell 1977). Figure 1(a) shows whispering-gallery rays – actually doubled rays – of frequency 3.2 kHz (respectively 14.2 kHz) starting at latitude $\lambda = -60°$ (respectively $\lambda = -55°$); the latter exhibits a 'beak' near the point where the local gyrofrequency is close to the ray frequency and its downgoing part corresponds to a quasiresonant propagation regime with $\kappa < 0.2$ near the equator. The spatial difference between the two variants of calculation is rather small and not visible on the figure; the time distortion (i.e. the relative difference in arriving time for almost-coinciding rays) is less than 10% along the trajectories. In Fig. 1(b) one can see a couple of doubled rays with frequency $\omega = 5.2$ kHz: a whispering-gallery doubled ray starting at $\lambda = -55°$ and a typical magnetospherically reflected (MR) doubled ray bouncing between LHR reflection points in the plasmasphere after coming close to the plasmapause (starting at $\lambda = -60°$); as in the previous case, the two variants almost coincide and the time distortion is around 10%. Finally Fig. 1(c) presents another couple of doubled rays: the first starts at $\lambda = -55°$ with $\omega = 7.2$ kHz and escapes from the plasmasphere near the equator, whereas the second ($\omega = 13.8$ kHz) turns down inside the plasmapause; the corresponding time distortion is roughly 20%. One should note that the similarity between rays calculated with the two dispersion laws is directly connected with the good coincidence between corresponding variations of coefficients χ and $\cos^2 \theta_R$ as functions of space coordinates, for a fixed frequency in the relevant frequency domain. However, to obtain a good coincidence between doubled rays after the low-altitude reflection point – as can be seen in Fig. 1(c) – requires a significant increase in the numerical accuracy of calculations using the total dispersion law (but not the modified one).

Whereas in most cases trajectories do not differ when calculated with the modified or the total dispersion laws, in a few cases a spatial distortion appears that increases with time, as one can see in Fig. 1(d). This is typical of adjacent trajectories (i.e. those lying at the boundary between qualitatively different kinds of rays) with small differences in starting parameters (or, as here, calculated with different dispersion laws), which, in spite of their close initial conditions, can have very different behaviour – for example, they can undergo trapping or free propagation. In these cases, one should not expect a quantitative coincidence of trajectories. At the same time, the contribution of such rays to spectrograms can be supposed to be vanishing and non-regular owing to their high variability with small changes of background plasma parameters. For illustration, Fig. 1(d) presents ray trajectories with very close frequencies ($\omega = 7.405$ kHz and $\omega = 7.4$ kHz). The ray at

https://doi.org/10.1017/S0022377801001301 Published online by Cambridge University Press

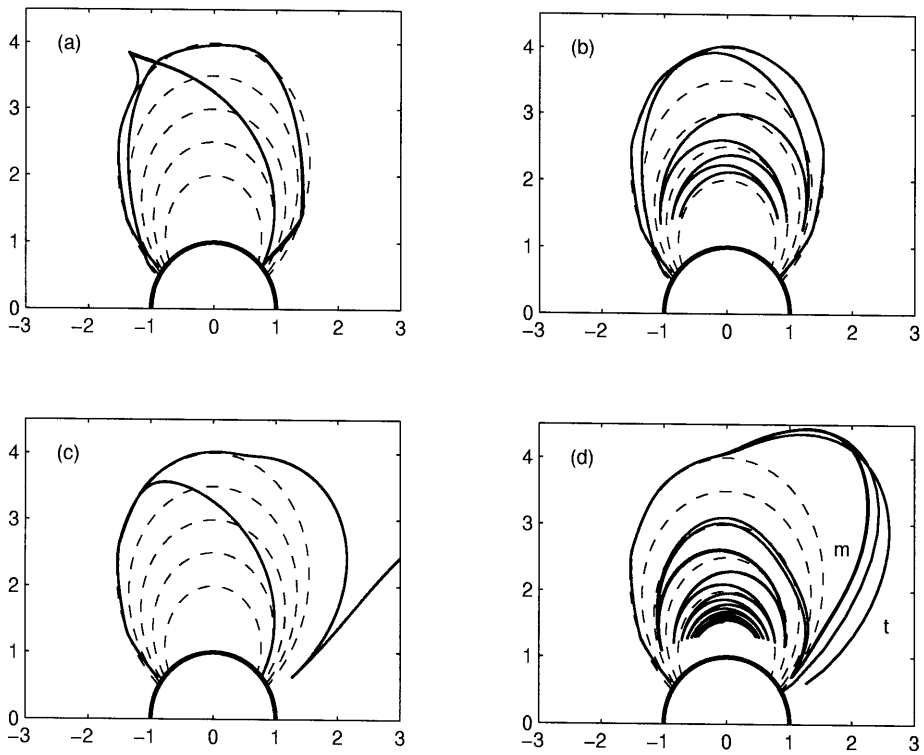

Figure 1. Typical whistler ray trajectories obtained by numerical calculations; the Earth is sketched as a half circle in thick solid lines; magnetic field lines are represented by dashed lines up to $L = 4$; on both axes, the coordinate is the distance to the Earth's centre normalized by the Earth's radius R_E; trajectories are sketched as solid lines. Doubled rays are represented, corresponding to simulations using the modified whistler dispersion law and the total one; when both rays constituting the so-called doubled ray can be distinguished from each other, they are labelled respectively by 'm' and 't', indicating whether the modified or the total dispersion law was used, respectively. (a) A whispering-gallery doubled ray starts at latitude $\lambda = -60°$ with frequency $\omega = 3.2\,\mathrm{kHz}$ and propagates near the plasmapause; the other starts at $\lambda = -60°$ with $\omega = 14.2\,\mathrm{kHz}$ and, after propagation in the captured regime near the plasmapause, exhibits a 'beak' near the point where the local gyrofrequency is close to the ray frequency. (b) shows a whispering-gallery doubled ray launched at $\lambda = -60°$ and a typical magnetospherically reflected (MR) doubled ray starting at $\lambda = -55°$ and bouncing between LHR reflection points with decreasing L-shell, both with frequency $\omega = 5.2\,\mathrm{kHz}$. (c) One doubled ray starts at $\lambda = -55°$ with $\omega = 7.2\,\mathrm{kHz}$ and escapes from the plasmasphere near the equator, whereas the second ($\omega = 13.8\,\mathrm{kHz}$) turns down inside the plasmapause before the equator. (d) Sensitivity to variation of starting conditions is demonstrated for doubled rays of very close frequencies ($\omega = 7.405\,\mathrm{kHz}$ and $\omega = 7.40\,\mathrm{kHz}$), both starting at $\lambda = -55°$; the modified dispersion law finally provides feeding of the plasmasphere by the MR whistler wave with frequency $\omega = 7.405\,\mathrm{kHz}$; however, calculations based on the total dispersion law (see the rays labeled by 't') show visible differences with respect to former trajectories (labeled by 'm'), even when calculations are performed with very high numerical accuracy.

$\omega = 7.405\,\mathrm{kHz}$ and governed by the modified dispersion law is finally captured by the plasmasphere; however, the ray trajectories corresponding to the total dispersion law differ visibly from each other just after escaping the plasmasphere, and are clearly different from the former ones even when calculations are performed with very high numerical accuracy.

https://doi.org/10.1017/S0022377801001301 Published online by Cambridge University Press

Finally, we want to stress that, no matter if distortion can sometimes be found for rays calculated with the two dispersion laws, the main qualitative features of spectrograms simulated by the two variants should be identical, since in both cases the same qualitatively different sets of rays play the same basic roles in the formation of spectral features. Then, numerical simulation of spectrograms can be an appropriate tool for determining large-scale space plasma features that essentially influence the rays' propagation properties; moreover, the use of the modified whistler dispersion law is an appropriate approach that takes into account the fact that space plasma parameters are not known exactly along the ray paths.

3.1.1. Propagation of magnetospherically reflected whistlers. This subsection illustrates one of the possible useful applications of the simplified dispersion law by considering the numerical simulation of the well-known spectrograms (i.e. frequency-time dynamical spectra) of so-called magnetospherically reflected (MR) whistlers. Such spectra (similar to that presented in Fig. 2), which are commonly observed near the equator on board high orbiting satellites (at altitudes of around two Earth radii), result from the propagation through the magnetospheric plasma of electron whistler waves emitted by lightning discharges and penetrating into the upper ionosphere within a rather wide latitude range (of around 20°) after a swift propagation below the ionosphere from the lightning source location. MR whistlers were first observed by the OGO 1 and 3 satellites, and their frequency–time spectral properties were discussed in detail by Smith and Angerami (1968) and explained numerically by Edgar (1976) (see also Shklyar and Jiricek 2000). These non-ducted whistlers propagate obliquely with respect to magnetic field lines in a smoothly inhomogeneous overdense plasmaspheric plasma, encountering successive geomagnetic L-shells during their bouncing back and forth between the Earth's hemispheres; reflections occur in space regions where the local lower-hybrid frequency is close to the frequency of the quasiresonant waves. Then, to each 'nose-type' line in the dynamic spectra registered by an equatorial satellite there corresponds a precise number of crossings of the equator by MR whistler rays before they reach the receiver.

Actually, MR whistler spectra are a remarkable manifestation of the electromagnetic filter property of the Earth's plasmasphere filled by a smoothly inhomogeneous plasma. As mentioned above, it is commonly accepted that the wave vector of starting whistler wave packets is oriented almost vertically. Then the two-dimensional continuum (finite interval of whistler frequencies excited by lightning discharges in a finite latitude domain under the ionosphere, if one ignores for simplicity the longitude coordinate when corresponding gradients are small enough) of simultaneously starting rays is transformed after propagation into a numerated set of lines in frequency–time spectra at some registration point. However, one must stress that, in order to reproduce visibly continuous lines in the calculated spectra, it is necessary to launch a huge amount of rays, because most of them do not reach the remote receiver. Then it is essential to find a way to significantly reduce computer time when calculating each ray path. This can be achieved by using the simplified whistler dispersion law to calculate ray propagation. Figure 2 shows an example of a whistler frequency–time spectrogram calculated using the simplified dispersion law; for comparison, when all terms are taken into account in the whistler dispersion relation for a cold plasma, similar results are obtained, but the total computing time is increased by at least 30% (and more if higher numerical accu-

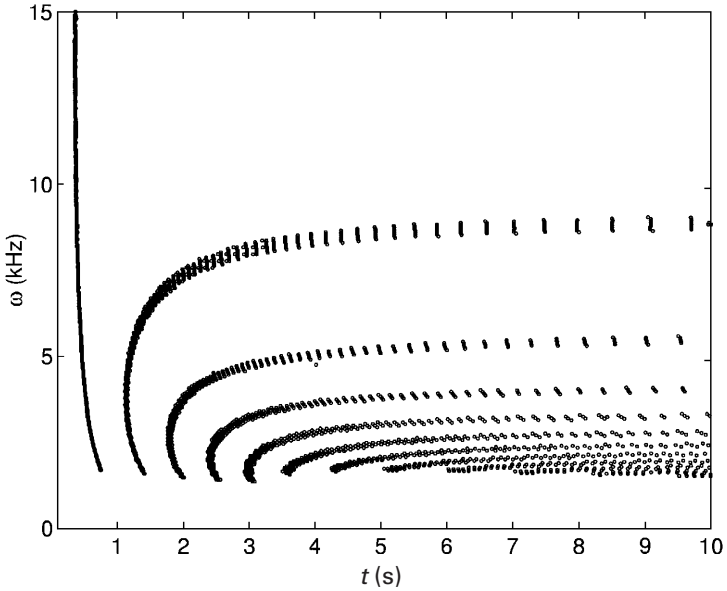

Figure 2. Typical frequency–time spectrogram of magnetospherically reflected whistlers calculated using the simplified wave dispersion law: whistlers with frequencies 1 kHz $< \omega <$ 20 kHz are emitted by a lightning source and enter the magnetosphere within an extended latitude domain ranging from $\lambda = -55^\circ$ to $\lambda = -20^\circ$; rays are launched with steps of $\Delta\lambda = 0.3^\circ$ in latitude and $\Delta\omega = 0.05$ kHz in frequency. The altitude of the satellite receiver is $h \simeq 9700$ km; the time of registration is indicated in seconds on the horizontal axis.

racy is required to achieve correct calculations), whereas the numerical stability is significantly decreased.

In general, the main reason for using an appropriately simplified dispersion law is not to determine with high accuracy all the parameters of the rays. Indeed, attention can be paid to the interesting possibility of revealing correspondences between the qualitative features of space plasmas crossed by the wide variety of ray paths reaching the 'receiver' and the calculated spectrogram features. One can expect that spectral features simulated using the simplified dispersion law should be correct (i.e. 'topologically' the same as those obtained using the total dispersion law) if the same sets of qualitatively different groups of rays can be reproduced in both approaches under the same background plasma conditions and with non-identical but close starting parameters – and this is our case, as has been demonstrated above. Then, the revelation of persistent spectral features after numerical enumeration of various space plasma characteristic parameters can be a promising basis for interpreting actually observed spectrograms. The exact numerical modelling of wave propagation phenomena is a rather obscure aim, since plasma parameters along ray paths are actually rather poorly defined.

4. Conclusions

The possibility has been shown of deriving a modified dispersion law for the electron whistler mode waves in a cold plasma that is valid for a wide range of ratios ω_c/ω_p of electron gyro- to plasma frequencies (see (13) and (14)) if the wave frequency is much less than ω_p and essentially exceeds the gyrofrequency of the lightest ion. This dispersion law is useful for efficient analytical treatment as well as for simplified

https://doi.org/10.1017/S0022377801001301 Published online by Cambridge University Press

and fast numerical calculations of wave propagation in a background plasma with high variability of characteristic parameters along wave-packet trajectories.

Moreover, the modified dispersion law retains the features of the total whistler dispersion equation in very wide frequency domains, that is, from the range of the lower-hybrid resonance frequency ω_{lhr} until the domain where ion motion can be neglected. In this frequency domain, the net combined contribution of ions can be expressed through the value of the lower-hybrid resonance frequency only. The conventional electron whistler dispersion law (20) (Shafranov 1967) is the natural limit of the modified law under overdense plasma conditions, i.e. $\omega_p \gg \omega_c$, and in the high-frequency range where the ion contribution can be omitted.

Test simulations of dynamical (frequency–time) spectra of whistler waves propagating in the Earth's plasmasphere after excitation by lightning discharges in wide frequency ranges and extended space regions under the ionosphere reveal that modern personal computers permit one to approach a solution of the so-called 'aiming' problem of the geometrical-optics equations by use of direct enumeration for starting conditions of whistler rays. Numerical studies have shown that, on average, the computing time of ray-tracing simulations is halved and that the numerical stability (as well as the frequency conservation accuracy) is significantly increased when using the simplified dispersion law instead of the total one. Moreover, the use of an appropriately simplified dispersion law that allows stable and fast numerical calculations constitutes a promising basis for investigating correspondences between plasma features along ray paths in extended space regions and persistent spectral features of spectrograms registered by remote receivers.

Acknowledgements

The authors acknowledge the Centre National de la Recherche Scientifique (CNRS, PICS 1310), France, the Institut Universitaire de France, Paris, NATO (PST.CLG.976896) and the Russian Academy of Sciences for their financial support. The research described in this publication was also made possible by Grants No. 98-05-65025a and No. 01-05-22003 from the Russian Foundation for Basic Research. Useful discussions with N. I. Bud'ko and D. R. Shklyar are also acknowledged.

Appendix. Group velocities, frequency gradients and dispersion features

The components of the group velocity $\mathbf{v}_g = (v_{g1}, v_{g2}, v_{g3})$ can be calculated using the dispersion law (12) as follows:

$$v_{g3} = \frac{\partial\omega}{\partial k_3} = \frac{k_3}{k} U(1 - V + \Delta \sin^2\theta), \tag{A 1}$$

$$v_{g1,2} = \frac{\partial\omega}{\partial k_{1,2}} = -\frac{k_{1,2}}{k} U(V + \Delta \cos^2\theta), \tag{A 2}$$

$$\Delta \equiv -\frac{\chi}{N^2} = \frac{\omega^2}{\Omega_c^2}\,\kappa\left(-\frac{\mu}{1+\mu} + \frac{\omega_{lhr}^2}{\omega^2}\right),$$

with

$$U = \frac{\Omega_c^2}{\omega^2[(1+\kappa)(1+\tilde{\kappa}) + \mu\tilde{\kappa}\cos^2\theta]}\,\frac{\omega}{k}, \tag{A 3}$$

https://doi.org/10.1017/S0022377801001301 Published online by Cambridge University Press

$$V = \frac{\omega^2}{\Omega_c^2}\left(1 - \frac{\omega_{lhr}^2}{\omega^2} - \kappa\tilde{\kappa}\right), \tag{A 4}$$

where v_{g3} is directed along the magnetic field and $v_{gi} (i = 1, 2)$ correspond to transverse components; k is the modulus of the wave vector $\mathbf{k} = (k_1, k_2, k_3)$; $N, \omega, \theta, \chi, \mu$, $\Omega_c, \omega_{lhr}, \kappa$ and $\tilde{\kappa}$ are defined in the text.

The frequency gradient can be written as

$$\begin{aligned} -\frac{\boldsymbol{\nabla}\omega^2}{\omega^2}&[(1+\kappa)(1+\tilde{\kappa}) + \mu\tilde{\kappa}\cos^2\theta] \\ &= (1+\kappa)\left(-\frac{\boldsymbol{\nabla}\omega_{lhr}^2}{\omega^2} + \tilde{\kappa}\frac{\boldsymbol{\nabla}\Omega_p^2}{\Omega_p^2}\right) \\ &\quad + \left(1 - \frac{\omega_{lhr}^2}{\omega^2} + \tilde{\kappa}\right)\left[\tilde{\kappa}\frac{\boldsymbol{\nabla}\Omega_p^2}{\Omega_p^2} - (1+\tilde{\kappa})\frac{\boldsymbol{\nabla}\Omega_c^2}{\Omega_c^2}\right] \\ &\quad - \tilde{\kappa}\cos^2\theta\left[(1+\mu)\frac{\boldsymbol{\nabla}\omega_{lhr}^2}{\omega^2} + \frac{\omega_{lhr}^2}{\omega^2}\left(\frac{\boldsymbol{\nabla}\Omega_p^2}{\Omega_p^2} - \frac{\boldsymbol{\nabla}\Omega_c^2}{\Omega_c^2}\right)\right], \end{aligned} \tag{A 5}$$

where Ω_p is defined by (8). A simple equation defines the frequency gradient near the LHR reflection point where $k_3 = 0$ and $\tilde{\kappa} = \omega_{lhr}^2/\omega^2 - 1$:

$$-\frac{\boldsymbol{\nabla}\omega^2}{\omega^2} = \frac{1}{1+\tilde{\kappa}}\left(-\frac{\boldsymbol{\nabla}\omega_{lhr}^2}{\omega^2} + \tilde{\kappa}\frac{\boldsymbol{\nabla}\Omega_p^2}{\Omega_p^2}\right). \tag{A 6}$$

The limit of high refractive index, $N^{-2} \ll 1$, described in the main text, can be obtained by omitting the terms containing Δ and $\mu\tilde{\kappa}$ in (A 1)–(A 4) as well as those containing $\cos^2\theta$ in (A 5).

Let us analyse the so-called Gendrin singularity point (Etcheto and Gendrin 1970) inherent to the conventional whistler dispersion law (20), which corresponds to the condition $|\mathbf{v}_{g\perp}| = 0$, or $\kappa = 1$. In this case, an electron moving with the resonant velocity $v_{3R} = c\omega_c/2\omega_p$ is in Cherenkov resonance with whistler wave packets of any frequencies $\omega = \frac{1}{2}\omega_c\cos\theta$ that have the same wavenumber $k = \omega_p/c$; then wave and particles move together, $|\mathbf{v}_{g\perp}| = 0$ and $v_{3R} = v_{g3}$, and the corresponding electron radiative energy loss tends to infinity.

However, the dependence of resonant velocity on wave frequency – inherent to (12) – can solve this 'infinity problem'. Indeed, in this case and for the high-frequency range $\omega \gg \omega_{lhr}$, the Gendrin singularity point corresponds to the condition $1 - \kappa\tilde{\kappa} - \mu\tilde{\kappa}\cos^2\theta \simeq 0$. Then, for finite μ, the wave packets move more slowly along the magnetic field than the resonant electrons:

$$v_{3R} - v_{g3} = \mu\tilde{\kappa}\frac{\omega^2}{\Omega_c^2}v_{3R}. \tag{A 7}$$

On the other hand, finite transverse leakage of wave energy out of the interaction region is provided for wave packets moving together with resonant electrons along the magnetic field ($v_{3R} = v_{g3}$); in this case, the transverse group velocity $v_{g\perp}$ is proportional to μ:

$$v_{g\perp} = \mu\tilde{\kappa}\frac{\omega^2}{\Omega_c^2}\frac{k_\perp}{k}U. \tag{A 8}$$

https://doi.org/10.1017/S0022377801001301 Published online by Cambridge University Press

The singularity point of the spectral energy loss $dW/d\omega$ of electrons at Cherenkov resonance under the approximation in use depends on the frequency near the Gendrin singularity point (where $p \simeq 1$) according to

$$\frac{dW}{d\omega}\alpha\frac{1}{\sqrt{1-p+\frac{1}{2}p(1+\mu)(\omega_{lhr}/\omega)^2}}, \qquad p=\left(\frac{2v_{3R}\omega_p}{c\omega_c}\right)^2 \simeq 1, \tag{A 9}$$

Omitting the ion contribution to the dispersion law for $\omega \gg \omega_{lhr}$, one recovers the conventional Gendrin 'infinity problem' at $p = 1$; in this case, the energy loss integrated over frequency diverges. Thus, the 'infinity problem' cannot be solved without taking into account the ion contribution to the whistler dispersion while one omits the small terms $(\omega/\omega_p)^2 \ll 1$ as has been done throughout this paper.

References

Angerami, J. J. and Thomas, J. O. 1964 Studies of planetary atmospheres, 1. The distribution of electrons and ions in the Earth's exosphere. *J. Geophys. Res.* **69**, 4537.

Boswell, R. W. and Chen, F. F. 1997 Helicons – the early years. *IEEE Trans. Plasma Sci.* **PS-25**, 1229.

Bud'ko. N. I. 1985 On the capture of waves into the LHR waveguide in the upper ionosphere. In: *Investigations of the Structure and Wave Properties of the Near-Earth Plasma*. Moscow: IZMIRAN, p. 60 [in Russian].

Chen, F. F. and Boswell, R. W. 1997 Helicons – the past decade. *IEEE Trans. Plasma Sci.* **PS-25**, 1245.

Edgar, B. C. 1976 The upper- and lower-frequency cutoffs of magnetospherically reflected whistlers. *J. Geophys. Res.* **81**, 205.

Etcheto, J. and Gendrin, R. 1970 About the possibility of VLF Cerenkov emission in the ionosphere by artificial electron beams. *Planet. Space Sci.* **18**, 777.

Felsen, L. B. and Marcuvitz, N. 1973 *Radiation and Scattering of Waves.* Englewood Cliffs, NJ: Prentice-Hall.

Helliwell, R. A. 1965 *Whistlers and Related Ionospheric Phenomena.* Stanford University Press.

Helliwell, R. A. 1993 Forty years of whistlers. In: *Modern Radio Science 1993* (ed. H. Matsumoto). Oxford University Press, p. 189.

Inan, U. S. and Bell, T. F. 1977 The plasmapause as a VLF wave guide. *J. Geophys. Res.* **82**, 2819.

Kennel, C. F. and Petscheck, H. E. 1966 Limit on stably trapped particle fluxes. *J. Geophys. Res.* **71**, 1.

Kimura, I. 1985 Whistler mode propagation in the Earth and planetary magnetospheres and ray-tracing techniques. *Space Sci. Rev.* **42**, 449.

Kravtsov, Y. A. and Orlov, Y. I. 1980 *Geometrical Optics of the Inhomogeneous Media.* Moscow: Nauka.

Petrov, Yu., Becoulet, A. and Monakhov, I. 2000 Coupled full-wave and ray-tracing numerical treatment of mode conversion in a tokamak plasma. *Phys. Plasmas* **7**, 911.

Shafranov, V. D. 1967 *Electromagnetic Waves in Plasma.* In: *Reviews of Plasma Physics*, Vol. 3 (ed. M. A. Leontovich). New York: Consultants Bureau, p. 1.

Shklyar, D. R. and Jiricek, F. 2000 Simulation of nonducted whistler spectrograms observed aboard the MAGION 4 and 5 satellites, *J. Atmos. Solar Terr. Phys.* **62**, 347.

Smith R. I. and Angerami, J. J. 1968 Magnetospheric properties deduced from Ogo 1 observations of ducted and nonducted whistlers. *J. Geophys. Res.* **73**, 1.

Stix, T. H. 1992 *Waves in Plasmas.* College Park, MD: American Institute of Physics.